Available online at www.sciencedirect.com

ScienceDirect

IFAC Papers Online CONFERENCE PAPER ARCHIVE

IFAC PapersOnLine 50-1 (2017) 12582–12587

Cooperative Adaptive Cruise Control for Vehicle Following During Lane Changes ⋆

Klaus W. Schmidt *

* *Mechatronics Engineering Department, Çankaya University, Ankara, Turkey (e-mail: schmidt@cankaya.edu.tr).*

Abstract: This paper addresses the longitudinal vehicle behavior before and during lane changes. Hereby, it is desired that the lane-changing vehicle simultaneously follows its predecessors on the lanes before and after the lane change. Specifically, the lane changing vehicle should keep a safe distance to the rearmost predecessor vehicle, while maintaining a small inter-vehicle spacing and supporting driving comfort. To this end, the paper develops an extension of cooperative adaptive cruise control (CACC). Instead of following a single vehicle as in the classical realization of CACC, it is proposed to follow a virtual vehicle that is evaluated based on distance measurements and communicated state information from the predecessor vehicles. A simulation study demonstrates the practicability of the proposed method.

Keywords: Autonomous vehicles, cooperative adaptive cruise control, lane changes, vehicle following, safety.

1. INTRODUCTION

Cooperative Adaptive Cruise Control (CACC) is a recent technology for safe vehicle following at small inter-vehicle spacings, using distance measurements and state information communicated among vehicles (Rjamani and Shladover, 2001; Shladover et al., 2015; Dey et al., 2016). In the current literature, CACC is used in vehicle strings, where each vehicle stays on a fixed lane and follows a unique predecessor vehicle. In this setting, various methods for the CACC controller design are available such as in (Dunbar and Caveney, 2012; Naus et al., 2010; Ploeg et al., 2014; Kamal et al., 2014; Kianfar et al., 2014). Different from the existing setting, this paper considers the usage of CACC for controlling the longitudinal vehicle motion before and during lane changes. In this case, a vehicle needs to simultaneously follow the predecessor vehicles on its current lane and on its target lane. In particular, it is desired to smoothly follow the potentially changing rearmost predecessor vehicle at a safe inter-vehicle spacing.

This paper addresses the stated problem by extending CACC by a virtual vehicle (VV) model. The VV is supplied with reference trajectories that are computed based on distance measurements and state information received from the predecessor vehicles. It is guaranteed by design that the trajectory of the VV

- converges to the trajectory of the rearmost predecessor vehicle if the distance between the predecessor vehicles is large
- smoothly changes between the predecessor vehicles if the predecessor vehicles overtake each other.

A simulation study shows that the lane-changing vehicle safely and smoothly follows the VV using CACC.

The safety of lane change maneuvers is studied in different contexts. Research works such as (Naranjo et al., 2008; Zheng et al., 2013; Nilsson et al., 2014; Du et al., 2015) consider trajectories for the combined longitudinal and lateral motion during a lane change. The human behavior during overtaking maneuvers is mimicked by fuzzy controllers in (Naranjo et al., 2008), respecting a safety distance to the vehicle to be overtaken. Zheng et al. (2013) generate a polynomial lane change reference path that is then tracked using model predictive control (MPC), whereby the reference path keeps a safe distance to the predecessor vehicle. High-level trajectory planning and low-level control of lane change maneuvers is realized by MPC by Nilsson et al. (2014). Hereby, a safe distance to the front and rear vehicles on the same lane is kept. Du et al. (2015) provide a mixed integer programming (MIP) formulation for planning a safe path that can be tracked by a PD controller. The MIP includes safety constraints for surrounding vehicles that are enforced for vehicles on the same lane as the lane changing vehicle. Different from the proposed method, these approaches consider safety only with respect to vehicles on the same lane as the lane changing vehicle. In addition, global position information is required when performing path tracking.

A different view is taken by Hatipoglu et al. (2003); Mukai and Kawabe (2006); Dang et al. (2015). Here, it is assumed that the longitudinal and lateral motion during a lane change can be considered separately. Accordingly, Hatipoglu et al. (2003) realize the longitudinal motion by intelligent cruise control and focus on the generation of steering commands for the lateral motion. Mukai and Kawabe (2006) address the longitudinal motion and propose a method for the high-level trajectory planning based on hybrid system modeling and model-predictive control (MPC) without a low-level realization. Hereby, the safety distance to two surrounding vehicles is taken into account.

⋆ This work was supported by the Scientific and Technological Research Council of Turkey (TUBITAK) [Award 115E372].

10.1016/j.ifacol.2017.08.2199

An extension of adaptive cruise control (ACC) to the case of lane changes is proposed by Dang et al. (2015). In this work, the scenario where the lane-changing vehicle has to simultaneously follow two vehicles on different lanes is addressed. Safe following is achieved by a combination of MPC and fuzzy logic based on distance measurements. This is different from our paper, where vehicle following is realized by CACC, which requires the usage of a virtual predecessor vehicle that provides consistent virtual distance measurements and additional state information.

The remainder of the paper is organized as follows. Section 2 provides the necessary background on CACC and Section 3 motivates the problem of simultaneously following two predecessor vehicles. In Section 4, the virtual vehicle is defined and its properties are demonstrated. Conclusions are given in Section 5.

2. PRELIMINARIES

2.1 Vehicle Following

This paper employs vehicle following as depicted in Fig. 1 based on the concept of *cooperative adaptive cruise control* (CACC) (Shladover et al., 2015; Liu and Xu, 2015; Ploeg et al., 2015; Dey et al., 2016).

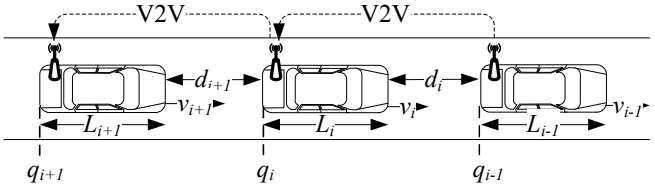

Fig. 1. Vehicle string with CACC.

For each vehicle i, we consider the *rear bumper position* q_i, the *length* L_i, the *velocity* v_i and the *inter-vehicle spacing* between vehicle i (front bumper) and $i-1$ (rear bumper)

$$d_i = q_{i-1} - q_i - L_i. \tag{1}$$

d_i is measured by Radar or LIDAR in analogy to adaptive cruise control (ACC). In addition, information from other vehicles can be received via vehicle-to-vehicle (V2V) communication. In this paper, we employ the frequently used *predecessor following* (PF) strategy, where vehicle $i-1$ sends state information to vehicle i (Ploeg et al., 2014; Shladover et al., 2015; Dey et al., 2016).

There are different policies for the desired vehicle spacing. We focus on the *constant-time-gap policy* with

$$d_{r,i} = r_i + h_i\, v_i \tag{2}$$

as the desired gap with the *headway time* h_i and the *desired spacing at standstill* r_i (for $v_i = 0$).

2.2 Control Architecture

We employ the control architecture in Fig. 3. G_i is the plant model of vehicle i with the transfer function

$$G_i(s) = \frac{Q_i(s)}{U_i(s)} = \frac{1}{(1 + s\,\tau_i)\,s^2}, \tag{3}$$

that is common in the recent literature (Ploeg et al., 2014, 2015). τ_i is the time constant of the *driveline dynamics*.

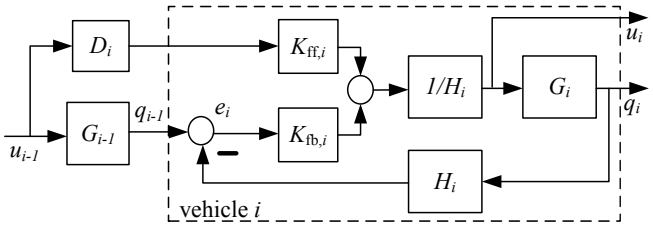

Fig. 3. Feedback loop for CACC on vehicle i.

The constant-time-gap policy in (4) is realized by the transfer function $H_i(s) = 1 + h_i\, s$ and the spacing error is

$$e_i = d_i - d_{r,i} = q_{i-1} - q_i - r_i - h_i\, v_i. \tag{4}$$

$K_{\mathrm{fb},i}$ is a feedback controller that controls the spacing error and $K_{\mathrm{ff},i}$ is a feedforward filter that receives the signal u_{i-1} from vehicle $i-1$ via V2V communication as in (Ploeg et al., 2014, 2015). Here, a communication delay represented by $D_i(s) = e^{-s\,\theta_i}$ is encountered.

3. FOLLOWING MULTIPLE VEHICLES: MOTIVATION AND REQUIREMENTS

3.1 Motivation

The usage of CACC in the existing literature is limited to the case where vehicles follow each other on a fixed lane, where the predecessor of each vehicle is uniquely known. However, this setting does not capture the desired vehicle behavior before and during lane changes, where the lane changing vehicle, denoted as *ego vehicle* (EV), is faced with predecessor vehicles on the lanes before and after the lane change. The EV needs to simultaneously follow both predecessor vehicles before and during the lane change.

In order to illustrate the stated scenario, we consider Fig. 2. Here, the EV intends to perform a lane change. Its two predecessor vehicles are L1 and L2. It is further assumed that EV can measure the distance to both L1 and L2 and receives u_{L1}, u_{L2} from L1, L2 via V2V communication. Part (a) shows the most basic configuration, where L1 and L2 assume the same position and travel at the same velocity. In that case, EV can alternatively perform CACC with L1 or L2. The situation is different in part (b) and part (c). In part (b), EV should follow the closer vehicle L1, whereas EV should follow L2 in part (c).

3.2 Safety and Comfort Requirements

We next point out the main issues when simultaneously following two vehicles. To this end, we perform a simple simulation experiment. L1 and L2 start at the same initial position with the same initial velocity 20 m/sec. L1 performs a speed-up/slow-down maneuver between the times 1 sec and 5 sec, whereas L2 performs a similar maneuver between the times 3.2 sec and 9 sec such that L2 overtakes L1 at time 6.2 sec. For illustration, we pursue a naive approach, where EV always performs CACC using the signals of the rearmost vehicle (RV). The simulation results are shown in Fig. 4. We plot the position, velocity and acceleration of L1, L2, RV and EV. Since velocities around 20 m/sec are chosen in the experiments, the figure shows "position$-20\,\mathrm{m/sec}\cdot t$" instead of the actual position for better visibility.

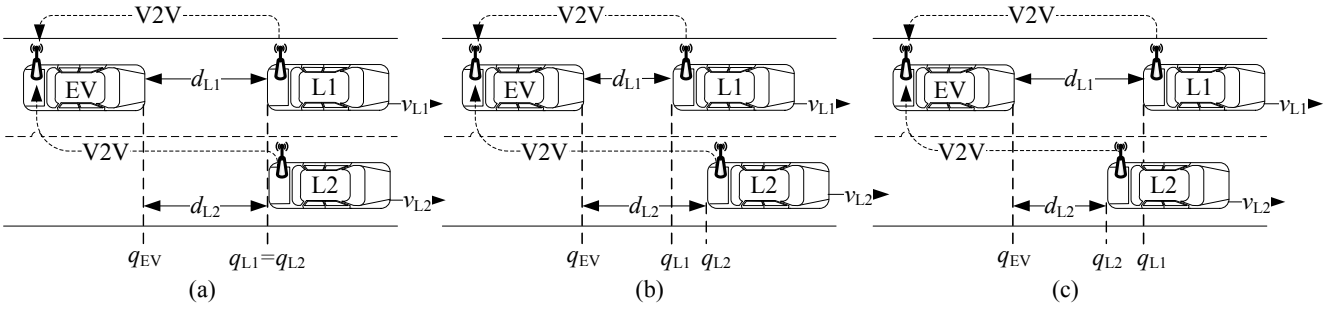

Fig. 2. Following multiple vehicles during/before a lane change.

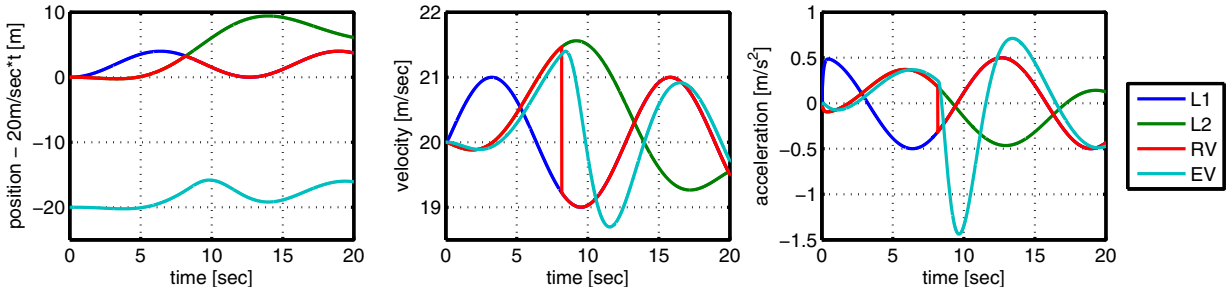

Fig. 4. Overtake maneuvers with switching of the leader vehicle.

Fig. 4 indicates that the naive approach can lead to undesired behavior. For example, a large spacing error of EV is observed after L2 overtakes L1, resulting in reduced driving safety (see Fig. 5). The reason for this effect is the velocity difference between L1 and L2 at the time of overtaking. EV first follows L2 with a larger velocity and then switches to L1 with a smaller velocity. In order to reduce the resulting spacing error, EV has to break sharply, which also reduces the driving comfort.

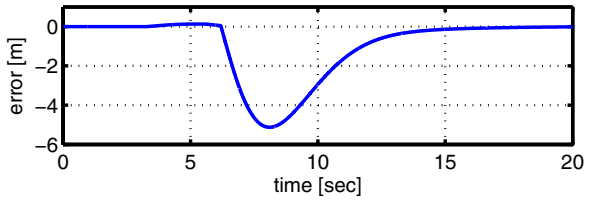

Fig. 5. Distance error signals of EV.

It has to be noted that the undesired behavior is observed due to the naive approach of directly following the RV. Nevertheless, the identified problem is general and needs to be addressed if the EV has to simultaneously follow two predecessor vehicles. In particular, a smooth transition should be achieved in case the RV changes to support driving safety and comfort. As opposed to the naive approach, this requires a fusion of the distance measurements with L1 and L2 as well as the communicated state information.

4. SIMULTANEOUS VEHICLE FOLLOWING USING A VIRTUAL VEHICLE

4.1 Virtual Vehicle Definition

We define a virtual vehicle (VV) that generates suitable signals for applying CACC on the EV. VV is based on the plant model in (3) as is shown in Fig. 6.

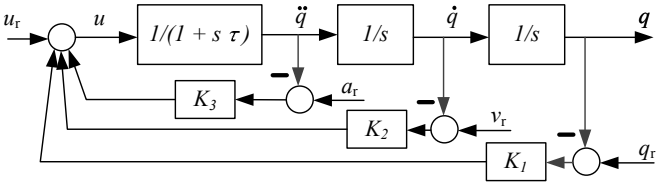

Fig. 6. Virtual vehicle realization.

Here, q and u denote the position and input signal of VV, respectively. In addition, VV employs reference signals q_r (position), v_r (velocity), a_r (acceleration) and u_r (input signal). These reference signals are computed based on the distance measurements $q_{i-1} - q_i$ and the communicated signals $\dot{q}_i$, $\ddot{q}_i$ and u_i, $i \in \{L1, L2\}$. The definition of suitable reference signals according to the observations in Section 3.2 is the main subject of the remainder of the paper. In order to track these reference signals, proportional feedback of the deviations $q_r - q$, $v_r - \dot{q}$ and $a_r - \ddot{q}$ is applied. From the implementation perspective, VV is computed locally by the EV and the signals u and q are used for performing CACC according to the architecture in Fig. 3.

4.2 Reference Position for the Virtual Vehicle

Considering the reference position q_r of VV, it is desired that $q(t) \leq \min\{q_{L1}(t), q_{L2}(t)\}$ in order to ensure driving safety. Let $\Delta q = q_{L1} - q_{L2}$ and $\overline{q}(t) = 0.5 \cdot (q_{L1}(t) + q_{L2}(t))$ be the position difference and average position of L1 and L2, respectively. Then, we define the reference position

$$q_r(t) = \overline{q}(t) + g_{\epsilon_q}(\Delta q)\,\Delta q \tag{5}$$

with a symmetric function $g_{\epsilon_q}(\Delta q) = -q_{\epsilon_q}(-\Delta q)$ such that

$$\begin{cases} g_{\epsilon_q}(\Delta q) = 0.5 & \text{if } \Delta q < -\epsilon_q \\ g_{\epsilon_q}(\Delta q) = -0.5 & \text{if } \Delta q > \epsilon_q \\ |g_{\epsilon_q}(\Delta q)| \leq 0.5 & \text{otherwise.} \end{cases} \tag{6}$$

Here, ϵ_q is a safety parameter that indicates if L1 and L2 are close to each other ($|\Delta q| \leq \epsilon_q$). Hence, $q_\mathrm{r}(t) = q_\mathrm{L1}(t)$ if L1 is sufficiently behind L2 ($\Delta q < -\epsilon_q$) and $q_\mathrm{r}(t) = q_\mathrm{L2}(t)$ in the reverse case ($\Delta q > \epsilon_q$). If both vehicles are close to each other ($-\epsilon_q \leq \Delta q \leq \epsilon_q$), a reference position close to the rearmost vehicle is assumed. Consider for example that L1 is the rearmost vehicle with $-\epsilon_q \leq \Delta q \leq 0$. Then, the distance between q_r and q_L1 is evaluated as

$$\begin{aligned} q_\mathrm{r}(t) - q_\mathrm{L1}(t) &= \frac{q_\mathrm{L1}(t) + q_\mathrm{L2}(t)}{2} + g_{\epsilon_q}(\Delta q(t))\Delta q(t) - q_\mathrm{L1}(t) \\ &= (g_{\epsilon_q}(\Delta q(t)) - 0.5)\,\Delta q(t). \end{aligned}$$

Hence, the maximum deviation from the desired minimum position $q_\mathrm{L1}(t)$ is given by

$$\Delta q_\mathrm{r,max} = \max_{-\epsilon_q \leq \Delta q \leq 0} (g_{\epsilon_q}(\Delta q) - 0.5)\,\Delta q. \tag{7}$$

Due to symmetry, the same result is obtained when considering L2 as the rearmost vehicle with $0 \leq \Delta q \leq \epsilon_q$.

In order to ensure a smooth transition for changes of the rearmost vehicle, we further require that $g_{\epsilon_q}(\Delta q)$ has three continuous derivatives w.r.t. Δq, that is, $g_{\epsilon_q}(\Delta q) \in C^3$, respecting that the vehicle model has degree three.

An example function for the stated requirements is

$$g_{\epsilon_q}(\Delta q) = \begin{cases} -1.25\,\frac{\Delta q}{\epsilon_q} + 2.5\,(\frac{\Delta q}{\epsilon_q})^3 - 2.5\,(\frac{\Delta q}{\epsilon_q})^4 + 0.75\,(\frac{\Delta q}{\epsilon_q})^5 & \text{if } \Delta q \geq 0 \\ -1.25\,\frac{\Delta q}{\epsilon_q} + 2.5\,(\frac{\Delta q}{\epsilon_q})^3 + 2.5\,(\frac{\Delta q}{\epsilon_q})^4 + 0.75\,(\frac{\Delta q}{\epsilon_q})^5 & \text{if } \Delta q < 0 \end{cases} \tag{8}$$

as depicted in Fig. 7 (a). It can be further seen in Fig. 7 (b), which shows $(q_\mathrm{r}(t) - \min\{q_\mathrm{L1}(t), q_\mathrm{L2}(t)\})/\epsilon_q$, that $\Delta q_\mathrm{r,max}$ in (7) depends on the chosen safety parameter ϵ_q. For example, $\Delta q_\mathrm{r,max} < 6\,\mathrm{cm}$ if $\epsilon_q = 1\,\mathrm{m}$ and $\Delta q_\mathrm{r,max} < 30\,\mathrm{cm}$ if $\epsilon_q = 5\,\mathrm{m}$.

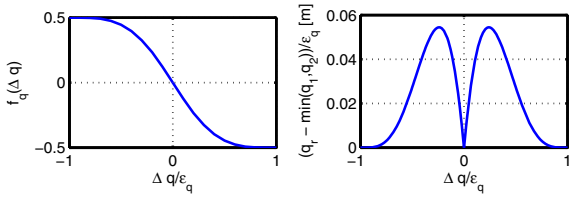

(a) (b)

Fig. 7. (a) Example choice of $g_{\epsilon_q}(\Delta q)$; (b) corresponding deviation from minimum position normalized by ϵ_q.

4.3 Reference Velocity for the Virtual Vehicle

Considering the reference velocity v_r, the velocity difference between L1 and L2 when performing an overtaking maneuver has to be taken into account as discussed in Section 3.2. For example, if L1 is the rearmost vehicle (see Fig. 2 (b)) and approaches L2 at a velocity $\dot{q}_\mathrm{L1} > \dot{q}_\mathrm{L2}$, it is desired that VV gradually adjusts its velocity from $\dot{q}_\mathrm{L1}$ to $\dot{q}_\mathrm{L2}$. Hereby, it is intuitive that more adjustment is needed if $|\Delta_q|$ is small or the velocity difference $|\Delta\dot{q}|$ is large.

In order to realize the specified requirements, we use a monotonically increasing function $\alpha_v(\Delta\dot{q})$ with $\alpha_v(0) = \epsilon_q$ that indicates the requirement of a velocity adjustment if $|\Delta q| < \alpha_v(\Delta\dot{q})$. Using α_v, we define the function

$$g_v(\Delta q, \Delta\dot{q}) = \begin{cases} g_{\epsilon_q}(\Delta q) & \text{if } |\Delta q| \geq \alpha_v(\Delta\dot{q}) \\ g_{\epsilon_q}(\Delta\dot{q})\,(1 - \frac{|\Delta q|}{\alpha_v(\Delta\dot{q})}) & \\ \quad + g_{\epsilon_q}(\Delta q)\frac{|\Delta q|}{\alpha_v(\Delta\dot{q})} & \text{otherwise} \end{cases} \tag{9}$$

and the reference velocity

$$v_\mathrm{r} = \dot{\overline{q}} + g_v(\Delta q, \Delta\dot{q})\,\Delta\dot{q}. \tag{10}$$

That is, if the distance $|\Delta q|$ between both predecessor vehicles is large compared to their velocity difference ($|\Delta q| \geq \alpha_v(\Delta\dot{q})$), v_r is equal to the velocity of the rearmost vehicle. Otherwise, v_r approaches the velocity of the slower vehicle especially for small ratios $|\Delta q|/\alpha_v(\Delta\dot{q})$. As an effect of the latter measure, VV is able to slow down if a faster rearmost vehicle is going to overtake a slower vehicle. In particular, a faster slow-down is achieved for larger velocity differences $\Delta\dot{q}$ since $a_v(\Delta\dot{q})$ is assumed to be monotonically increasing. For illustration, Fig. 8 shows $g_v(\Delta q, \Delta\dot{q})$ for $\epsilon_q = 1\,\mathrm{m}$ and $a_v(\Delta\dot{q}) = 1 + 0.3 \cdot \Delta\dot{q}^2$.

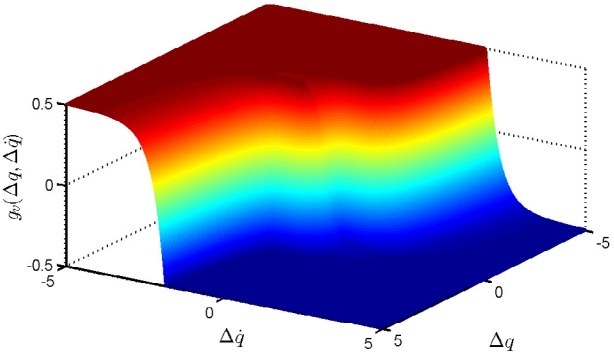

Fig. 8. Example choice of $g_v(\Delta q, \Delta\dot{q})$.

4.4 Reference Acceleration/Input for the Virtual Vehicle

Considering the reference acceleration/input, we require that a_r and u_r follow the respective signal of the rearmost vehicle with a smooth transition in case of overtaking similar to the reference position in Section 4.2. That is,

$$a_\mathrm{r}(t) = \ddot{\overline{q}}(t) + g_{\epsilon_q}(\Delta q)\,\Delta\ddot{q} \tag{11}$$

and

$$u_\mathrm{r}(t) = \overline{u}(t) + g_{\epsilon_q}(\Delta q)\,\Delta u \tag{12}$$

using $\overline{u}(t) = \dfrac{u_\mathrm{L1}(t) + u_\mathrm{L2}(t)}{2}$ and $\Delta u = u_\mathrm{L1}(t) - u_\mathrm{L2}(t)$.

4.5 Virtual Vehicle Properties

It is now possible to state two main properties of the VV defined in the previous sections.

Theorem 1. Assume that the VV is defined as in Section 4.1 with the reference signals in (5), (9), (11) and (12). Further let K_1, K_2, K_3 be chosen such that $\tau\,s^3 + (K_3 + 1)\,s^2 + K_2\,s + K_1$ is Hurwitz. Then, it holds that

1. $\lim_{t\to\infty} q(t) = \min\{q_\mathrm{L1}(t), q_\mathrm{L2}(t)\}$ if $\Delta q(t) \geq a_v(\Delta\dot{q}(t))$
2. $\lim_{t\to\infty} q(t) - \min\{q_\mathrm{L1}(t), q_\mathrm{L2}(t)\} \leq \Delta_\mathrm{r,max}$ if $\Delta\dot{q} = \Delta\ddot{q} = \Delta\dddot{q} = 0$.

The proof of Theorem 1 is published in the form of a technical report. Theorem 1 characterizes two important scenarios for the trajectory q of VV. According to 1., q equals the trajectory of the rearmost vehicle if the distance between both predecessor vehicles is sufficiently large. Furthermore, 2. suggests that q is close to the trajectory of the rearmost vehicle if both leader vehicles travel at the same constant velocity. We further note that the computation of the VV trajectory does not require any optimization and is hence suitable for a real-time implementation. In order to evaluate the dynamic behavior of the VV in scenarios different from the ones in Theorem 1, we next perform various simulation experiments.

4.6 Simulation Examples

We consider the setting in Fig. 2 with two predecessor vehicles L1 and L2 and the EV that follows VV according to Section 4.1. We perform three different experiments. In each experiment, we plot the position, velocity and acceleration of L1, L2, VV and EV as well as the spacing error of EV according to (4). Since velocities around 20 m/sec are chosen in the experiments, our plots show "position $-$ 20 m/sec $\cdot\, t$" instead of the actual position. We use a plant model with $\tau = 0.1$ and the headway time constant is $h = 0.5$ as in (Ploeg et al., 2014). For the realization of the reference trajectories, we use $g_{\epsilon_q}(\Delta q)$ in (8), $\epsilon_q = 1\,\text{m}$ and $a_v(\Delta\dot{q}) = 1 + 0.3 \cdot \Delta\dot{q}^2$. The feedback constants in Fig. 6 are chosen as $K_1 = 10$, $K_2 = 30$ and $K_3 = 25$ such that $\tau\, s^3 + (K_3+1)\, s^2 + K_2\, s + K_1$ is Hurwitz.

The first experiment is identical to the experiment in Section 3.2, using VV instead of RV for CACC. The simulation results are shown in Fig. 9. It is readily observed that VV moves close to the position of the rearmost vehicle. In particular, $q \approx q_{\text{L2}}$ until L2 overtakes L1 at time 6.2 sec and $q \approx q_{\text{L1}}$ afterwards. This behavior is enabled by the realization of v_{r} in (10). As can be seen from the figure, the velocity of VV decreases before the actual overtaking maneuver, achieving a smooth transition when the rearmost vehicle changes. In addition, it can be seen that the EV is able to follow VV (and hence the rearmost vehicle) at a safe distance using CACC with the virtual input signals u and q from VV. This observation is confirmed when looking at the spacing error according to (4) in Fig. 11, which stays below 1 m for this experiment. We recall that a spacing error with a magnitude of up to 5 m is observed in Fig. 5 when using the RV for CACC.

The second experiment is analogous to the first experiment with the difference that L2 overtakes L1 at time 8.6 sec with a lower speed difference. The results are shown in Fig. 10. Again, the VV slows down before overtaking, whereby smaller accelerations are required compared to experiment 1 and smaller spacing errors are encountered (see Fig. 11).

The third experiment in Fig. 12 realizes multiple overtake maneuvers with non-zero accelerations, where the overtaking vehicle accelerates and the vehicle being overtaken decelerates. Similar to the previous experiments, a smooth transition between changing RV trajectories with small spacing errors is achieved.

We note that the VV is defined for the case of zero communication delay $\theta_i = 0$ according to Fig. 3. In order to provide a preliminary assessment of the case with non-zero communication delay, we consider the same setting as in experiment 1 to 3, whereby the communicated signals $\dot{q}_i$, $\ddot{q}_i$, u_i, $i \in \{\text{L1}, \text{L2}\}$ are received with a delay of $\theta = 0.06$ sec as in (Naus et al., 2010). The resulting spacing errors are also shown in Fig. 11. It can be seen that the suggested VV shows robustness to communication delays. A further investigation of this topic is the subject of future work.

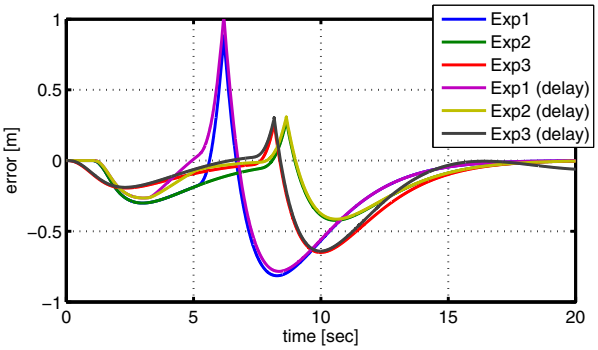

Fig. 11. Spacing error signals of EV for three experiments.

5. CONCLUSION

Cooperative adaptive cruise control (CACC) is a recent technology for safe vehicle following at small inter-vehicle spacings based on distance measurements and communicated state information. This paper extends CACC to the case where a vehicle follows two predecessor vehicles on different lanes simultaneously, for example when preparing or carrying out a lane change. To this end, the paper defines a virtual vehicle (VV) that can be used for safe and smooth vehicle following and that can be computed in real-time. On the one hand, VV tracks the trajectory of the rearmost predecessor vehicle if it is safe to follow this vehicle. On the other hand, a smooth transition between the predecessors is achieved in case they overtake each other. Representative simulation experiments demonstrate the applicability of the proposed method.

REFERENCES

Dang, R., Wang, J., Li, S.E., and Li, K. (2015). Coordinated adaptive cruise control system with lane-change assistance. *IEEE Transactions on Intelligent Transportation Systems*, 16(5), 2373–2383.

Dey, K.C., Yan, L., Wang, X., Wang, Y., Shen, H., Chowdhury, M., Yu, L., Qiu, C., and Soundararaj, V. (2016). A review of communication, driver characteristics, and controls aspects of cooperative adaptive cruise control (CACC). *IEEE Transactions on Intelligent Transportation Systems*, 17(2), 491–509.

Du, Y., Wang, Y., and Chan, C.Y. (2015). Autonomous lane-change controller. In *IEEE Intelligent Vehicles Symposium*, 386–393.

Dunbar, W. and Caveney, D. (2012). Distributed receding horizon control of vehicle platoons: Stability and string stability. *Automatic Control, IEEE Transactions on*, 57(3), 620–633.

Hatipoglu, C., Ozguner, U., and Redmill, K.A. (2003). Automated lane change controller design. *IEEE Transactions on Intelligent Transportation Systems*, 4(1), 13–22.

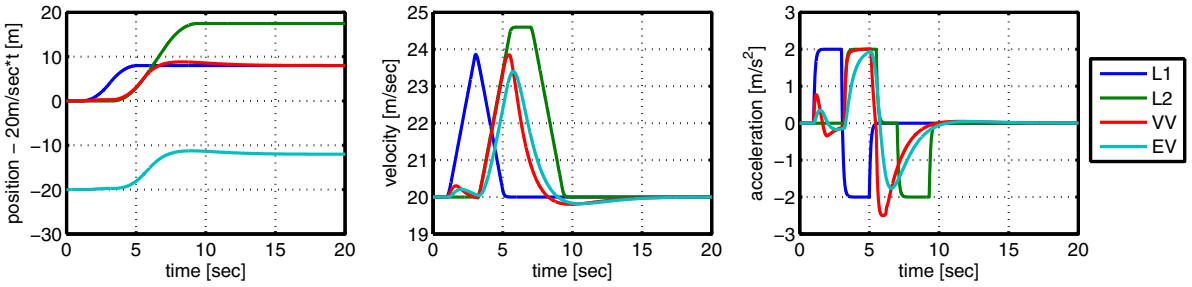

Fig. 9. Overtake maneuver with a large velocity difference of L1 and L2.

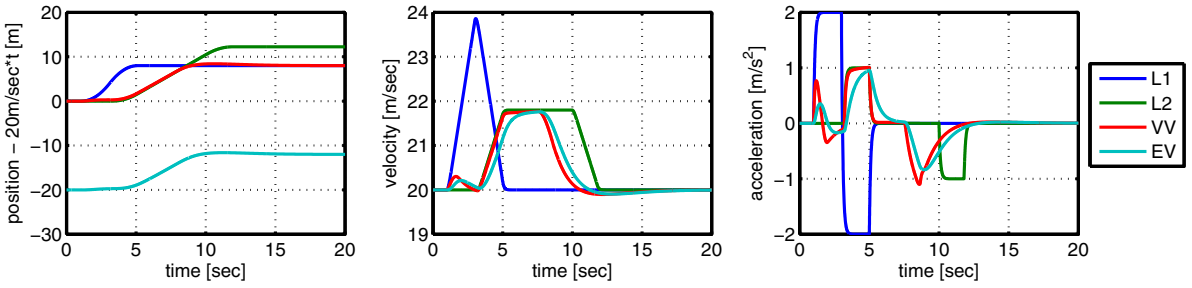

Fig. 10. Overtake maneuver with a small velocity difference of L1 and L2.

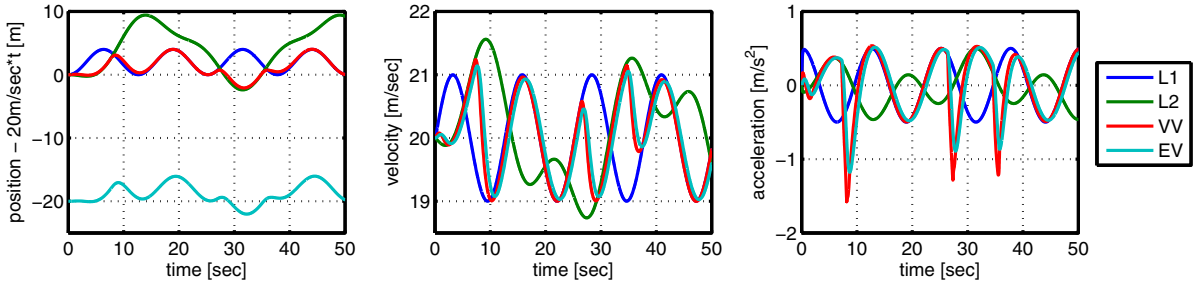

Fig. 12. Multiple overtake maneuvers at different velocity differences.

Kamal, M.A.S., i. Imura, J., Hayakawa, T., Ohata, A., and Aihara, K. (2014). Smart driving of a vehicle using model predictive control for improving traffic flow. *IEEE Transactions on Intelligent Transportation Systems*, 15(2), 878–888.

Kianfar, R., Ali, M., Falcone, P., and Fredriksson, J. (2014). Combined longitudinal and lateral control design for string stable vehicle platooning within a designated lane. In *Intelligent Transportation Systems, IEEE International Conference on*, 1003–1008.

Liu, Y. and Xu, B. (2015). Improved protocols and stability analysis for multivehicle cooperative autonomous systems. *IEEE Transactions on Intelligent Transportation Systems*, 16(5), 2700–2710.

Mukai, M. and Kawabe, T. (2006). Model predictive control for lane change decision assist system using hybrid system representation. In *SICE-ICASE International Joint Conference*, 5120–5125.

Naranjo, J.E., Gonzalez, C., Garcia, R., and de Pedro, T. (2008). Lane-change fuzzy control in autonomous vehicles for the overtaking maneuver. *IEEE Transactions on Intelligent Transportation Systems*, 9(3), 438–450.

Naus, G.J.L., Vugts, R.P.A., Ploeg, J., Van de Molengraft, M.J.G., and Steinbuch, M. (2010). String-stable CACC design and experimental validation: A frequency-domain approach. *Vehicular Technology, IEEE Transactions on*, 59(9), 4268–4279.

Nilsson, J., Gao, Y., Carvalho, A., and Borrelli, F. (2014). Manoeuvre generation and control for automated highway driving. In *IFAC World Congress*, 6301–6306.

Ploeg, J., Semsar-Kazerooni, E., Lijster, G., van de Wouw, N., and Nijmeijer, H. (2015). Graceful degradation of cooperative adaptive cruise control. *IEEE Transactions on Intelligent Transportation Systems*, 16(1), 488–497.

Ploeg, J., Shukla, D., Van De Wouw, N., and Nijmeijer, H. (2014). Controller synthesis for string stability of vehicle platoons. *Intelligent Transportation Systems, IEEE Transactions on*, 15(2), 854–865.

Rjamani, R. and Shladover, S.E. (2001). An experimental comparative study of autonomous and cooperative control systems for automated vehicles. *Journal of Transportation Research, Part C: Emerging Technologies*, 9(1), 15–31.

Shladover, S.E., Nowakowski, C., Lu, X.Y., and Ferlis, R. (2015). Cooperative adaptive cruise control: Definitions and operating concepts. *Transportation Research Record*, 2489, 145–152.

Zheng, H., Huang, Z., Wu, C., and Negenborn, R.R. (2013). *Model Predictive Control for Intelligent Vehicle Lane Change*, 265–276.